Pressure-Less Processing of Ceramics with Deliberate Elongated Grain Orientation and Size

Hortense Le Ferrand

Abstract Ceramics with heterogeneous microstructures have the potential to exhibit local variations in properties and unusual combinations of those, just like highly mineralized biomaterials do. However, to date, the microstructures achieved in technical and structural ceramics cannot rival the diversity and complexity of those found in biomaterials due to the lack of adapted processing methods. Recent research, however, demonstrated that local hardness and elastic modulus can be realized in alumina ceramics by controlling the orientation of the grains in periodically varying structures. This deliberate tuning of the grain orientation resulted from the magnetically-driven alignment of anisotropic template particles in the initial liquid suspension. During the sintering at high temperature, the template particles grew as anisotropic grains with the orientation set by the magnetic field. To expand the design freedom of such ceramics in terms of microstructure and properties, this paper aims at tuning the grain size, grain orientation, and final porosity of sintered alumina. The methodology to build multilayered ceramics using varying template particles sizes is described and examples of the microstructures obtained are provided. This work contributes to pushing forward the field of bioinspired ceramics that would hopefully give rise to structural ceramics with unusual combinations of local properties.

Keywords Microstructure · Ceramic · Grain growth · Magnetic orientation

H. Le Ferrand (✉)
School of Mechanical and Aerospace Engineering, School of Materials Science and Engineering, Nanyang Technological University, 50 Nanyang Avenue, Singapore 639798, Singapore
e-mail: hortense@ntu.edu.sg

B. Li et al. (eds.), *Advances in Powder and Ceramic Materials Science*,
The Minerals, Metals & Materials Series,
https://doi.org/10.1007/978-3-030-36552-3_5

Introduction

Heterogeneous structures in highly mineralized materials are desired to achieve local properties, customization, and unusual combinations of functions [1]. Such unusual combinations may be, for example, damage and impact resistance with high strength and hardness [2, 3], wear-resistance and lightweightness with strength, or functional gradients. These properties contrast with most conventional ceramics that generally aim at homogeneity and are largely inspired by many biological and highly mineralized materials [4, 5]. Indeed, many hard biocomposites exhibit local variations in chemical composition, density, and reinforcement orientation. A typical example of such natural materials is the dactyl club of the Mantis Shrimp [6]. This club combines strength with impact resistance by featuring multiple gradients from the outer to the inner part: a gradient in crystallinity and mineral phase from fluorapatite to amorphous calcium phosphate, a gradient in density with an increase in organic content, and a gradient in the pitch of a helicoidal arrangement of mineral rods [7]. Reproducing such complex microstructures in structural technical ceramics remains a challenge but is desired to expand the use of ceramics. Indeed, strong, hard, and tough lightweight materials find a large range of applications in the biomedical, aerospace, and automotive industries [8, 9].

Several paths have been explored to approach nature's microstructural complexity in porous systems and reinforced composites, using methods such as field-assisted freeze casting [10] or additive manufacturing [11]. The materials fabricated by these methods, however, do not reach the high strength, hardness, and toughness of their biological counterparts. To realize such mechanical properties, the microstructural control has to be done in a highly mineralized system [12]. Recently, the use of magnetic fields to control the orientation of elongated particles in any direction in space showed promising results in designing ceramics and composites with local properties [2, 13, 14]. In one of these processes, the magnetic orientation of microparticles in liquid is combined with two traditional ceramic processes, namely, slipcasting and templated grain growth (TGG) [13]. Typically, the method consists in aligning, using a magnetic field, anisotropic template microparticles co-suspended with smaller nanoparticles of the same composition in an aqueous solution. After drying, the template particles retain their orientation and during the sintering, they grow to form large anisotropic grains along this orientation [15, 16]. Using this method, dense alumina ceramics with deliberate orientation of their grains could be fabricated. In particular, periodically varying orientations could be achieved in a variety of geometrical shapes, to reproduce the pitch gradient found in the Mantis Shrimp dactyl club [13] (Fig. 1). The local hardness and moduli were found to vary along the pitch [13], as a consequence of the dependence of crystalline orientation and number of weak interfaces along the loading direction with the mechanical properties [17, 18].

To expand the degree of design freedom in such microstructures, as well as to increase the strength and toughness, additional control over the grain size and aspect ratio is desired. Indeed, extrapolating the theory of reinforced composites to

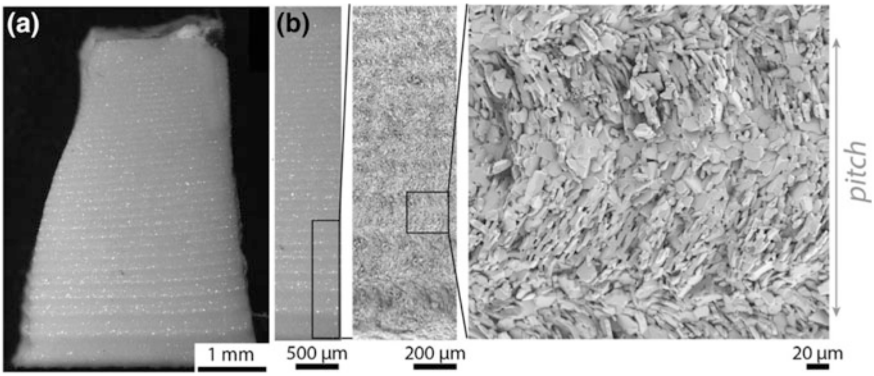

Fig. 1 Optical image of a periodically microstructured alumina ceramic (**a**) and electron microscopy images of its internal grain arrangement (**b**) prepared by magnetically-driven assembly and templated grain growth (reproduced from [13], copyright © 2019, Wiley and sons)

ceramics with aligned grains, hardness, and strength are expected to increase with the aspect ratio of the grains (Fig. 2a) [19]:

$$H_v = H_{v0} + H_{v1}\sqrt{L}, \tag{1}$$

where L is the width of the grain, H_v the hardness and H_{v0} and H_{v1} constants, and

$$\tau = \tau_0 + \tau_1\sqrt{L}, \tag{2}$$

where τ is the yield strength and τ_0 and τ_1 are constants. In addition, the fracture mode of highly textured materials changes from brittle where the grains break to pull-out mode where the grains deflect the crack at their interfaces [20]. As a result, aspect ratio along with grain dimension and orientation can be expected to influence the toughness of the material as well as the strength (Fig. 2b). Combining these

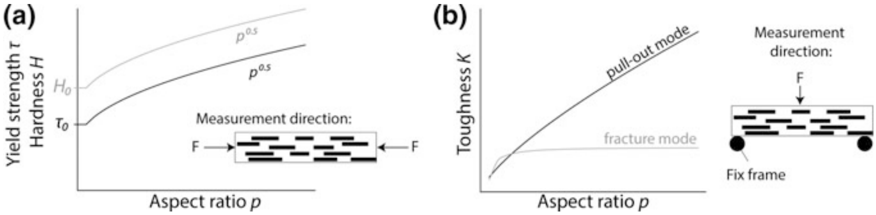

Fig. 2 Trends of the mechanical response of ceramics with anisotropic and aligned grains as a function of the aspect ratio of those grains: **a** Yield strength τ and hardness H for a load F applied along the long dimension of the grains, **b** toughness K in the case of a crack initiated perpendicularly to the alignment direction

multiple features could lead to enhanced and localized properties in structural ceramics.

To explore this design space and move one step forward in the direction of hard and tough lightweight materials, this paper describes the fabrication of multilayer alumina ceramics with controlled grain orientation and size, using the magnetically-assisted slipcasting and templated grain growth process (MASC-TGG). First, the influence of the geometrical dimensions of the initial anisotropic templates on the grain size and material porosity before and after sintering are described and compared to theoretical predictions. Then, those templates are functionalized to respond to external magnetic fields and biaxially align in arbitrary directions. Finally, an example of a multilayer ceramic with controlled grain size and orientation is presented. Such controlled microstructures could be used to design ceramic and composite materials that exhibit local properties, controlled crack path, and, therefore, enhanced strength and toughness. This work is a step forward in the design and fabrication of tough structural materials with applications in health, transport, or defense.

Materials and Methods

Slurry Preparation, Casting, and Sintering

Alumina microplatelets (Al_2O_3 pl, Kinsei Matec Co., Japan) were suspended at a ratio 1:1 in a waterborne and acidic dispersion of hydrophilic fumed alumina nanoparticles (Al_2O_3 np, AERODISP W 440, Evonik, Germany) containing 40 vol. % solids. The mixture was stirred overnight before being casted onto a gypsum substrate (Ceramix, Germany) prepared and dried earlier. After the absorption of the water from the slurry in the gypsum plaster, both sample and plaster were dried at mild temperature overnight (Binder VD 53, Fischer Scientific Pte Ltd, Singapore). The green bodies obtained were subsequently sintered in air (sintering furnace Nabertherm, Switzerland) with the following heating procedure: 5 °C/min up to 500 °C, plateau at 500 °C for 2 h, then up to 1600 °C in 6 h and plateau at 1600 °C for 2 h. The parameters for the theoretical determination of the grain growth were determined by varying the sintering temperature and applying the method described by Suvaci et al. [21].

Magnetic Response of Alumina Platelets

The alumina platelets were magnetized following a procedure described elsewhere [22]. Their magnetic response was observed under an optical microscope (Nikon Epiphot 200) in an aqueous solution of 5 wt% of polyvinyl pyrrolidone

(Sigma-Aldrich, China, MW = 360’000). The magnets used were rare-earth neodymium magnets (Eclipse, Switzerland) attached to DC motors (RS PRO, China). The images were recorded using the camera (Infinity, Lumenera) and software (Infinity) and analyzed using Image J (NIH, USA).

Characterization of the Ceramics

Green bodies and sintered ceramics were imaged using an electron microscope (FESEM 76000F, Japan). Green body samples were broken manually and coated with 5 nm of Pt. The sintered ceramics were polished and thermally etched at 1600 °C for 20 min before applying the Pt coating. The density of the samples was measured using the Archimedes principle, using toluene as a solvent (Sigma-Aldrich, India) for the green bodies and deionized water for the sintered samples.

Results and Discussion

Overview of the MASC-TGG Process

The combination of MASC with TGG was selected as the method of choice for the fabrication of ceramics with deliberate grain orientation and size (Fig. 3). Indeed, MASC-TGG is a pressure-less method that is suitable for near net-shape manufacturing [13]. The method consists in preparing a liquid suspension containing both anisotropic micron-scale particles and nanoparticles of the same chemistry, Al_2O_3 in this study. The micron-scale particles, also called platelets, are modified to respond to external magnetic fields [22]. This modification consists in adsorbing superparamagnetic iron oxide nanoparticles (Fe_3O_4 np) at their surface and has been developed elsewhere [22, 23]. When the suspension is liquid enough, the platelets can be oriented in any deliberate direction [2, 14]. Casting the suspension onto a porous mold, the liquid is slowly removed by capillary forces in a time-dependent manner [2]. As the water is removed, the viscosity rises, locking the orientation of the platelets in place (Fig. 3a). The larger particles will serve as templates to the smaller particles during the sintering at high temperature to lead to large anisotropic grain with the same geometric and crystalline orientations [15, 16]. This is the templated grain growth process that is used for the consolidation and densification of the ceramic (Fig. 3b).

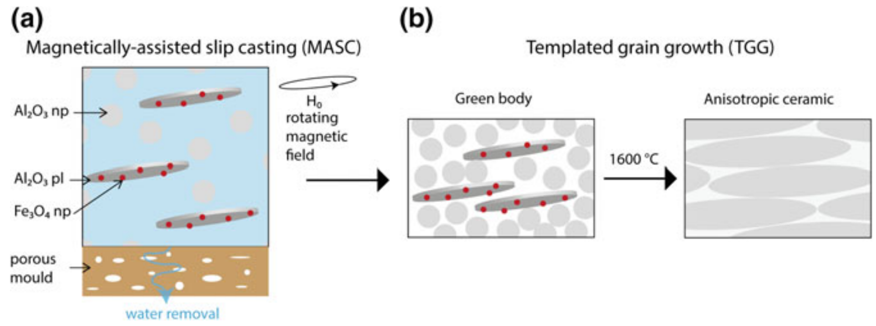

Fig. 3 Overview of the process used to fabricate the anisotropic ceramics, combining magnetically-assisted slipcasting (a, MASC) and templated grain growth (b, TGG). During MASC, magnetically responsive anisotropic alumina platelets (Al_2O_3 pl) decorated with iron oxide nanoparticles (Fe_3O_4 np) are co-suspended with alumina nanoparticles (Al_2O_3 np) in water. The platelets are oriented *via* a rotating magnetic field $\boldsymbol{H_0}$ as the liquid is removed through the pores of a mold made of plaster. The dry assembly called green body is then consolidated and densified into a ceramic by TGG at 1600 °C

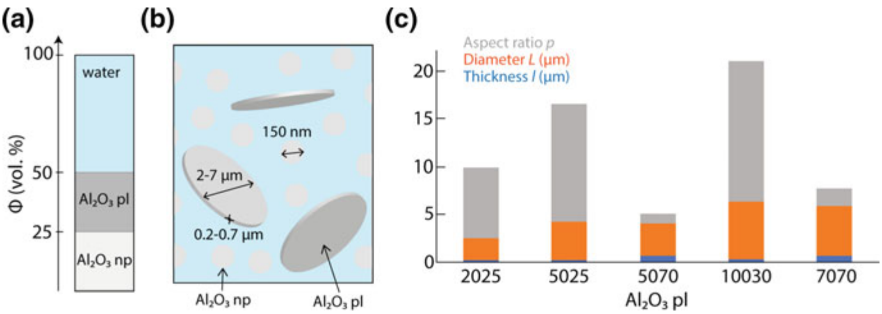

Fig. 4 **a** Composition of the slurry in terms of volume fraction, **b** schematics of the suspension and **c** geometrical dimensions of the Al_2O_3 pl used in the different slurries

Slurry Composition

The composition of the slurries was optimized for particles with the dimensions and aspect ratios used in this study (Fig. 4). The key property for the slurry preparation is to exhibit low viscosity while containing a concentration in solid high enough to maintain the particles orientations after drying [14]. To this aim, the Al_2O_3 platelets were added to a commercial suspension of alumina nanoparticles. The acidic pH around 4 allowed good dispersion. Tuning the concentration of the Al_2O_3 platelets, it was found that total solid concentrations below 50 vol.% lead to significant sedimentation of the platelets and warping of the casted samples after drying, for all the particle sizes used in this study. Furthermore, above 50 vol.% the viscosity was found to drastically increase, leading to the formation of a paste-like material.

In such high viscosity suspension, the platelets could not be aligned by a magnetic field. For the range of platelet sizes used herein the experiments, 50 vol.% total solid content was found suitable for the slurry preparation and was used in the remainder of the study. Using the same solid content for different particle sizes is convenient for the future processing of continuous gradients and to prevent distortions during drying.

Casting and Densification by TGG

The consolidation and densification of the green bodies into ceramics was achieved by templated grain growth as described earlier. The final grain dimensions and ceramic densities were found to depend on the initial platelet sizes (Fig. 5). Using the slurries containing 50 vol.% solid content, no significant deformation was observed after sintering of 3 mm-thick cylindrical samples. For all compositions, the microstructure showed elongated grains, oriented at random angles when no magnetic field is applied (Fig. 5a). The images also revealed the presence of pores suggesting that the packing of the nanoparticles around the platelets might also be affected by the aspect ratio of the platelets. The theory of the templated grain growth could be applied to the compositions to predict the final grain size (Fig. 5b), using the following equation [21]:

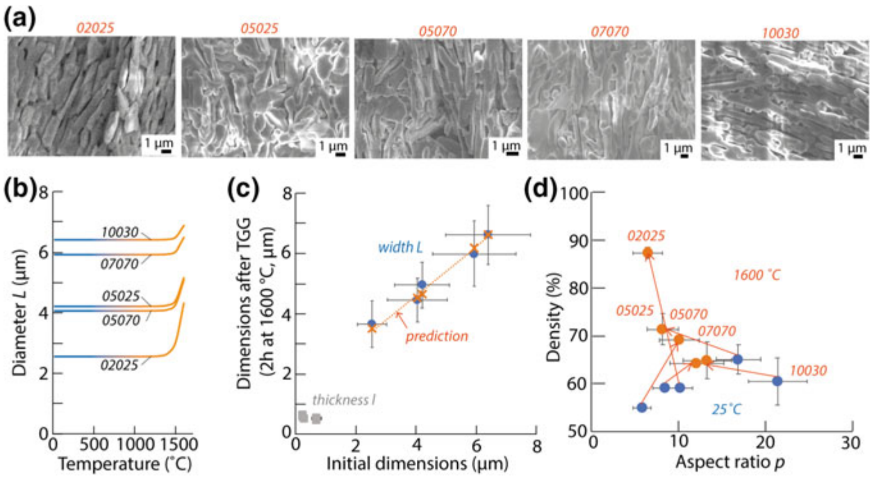

Fig. 5 **a** Electron micrographs of thermally etched cross sections of the ceramics prepared using the five different platelet dimensions. **b** Theoretical prediction of the grain growth *via* TGG. **c** Experimental and predicted dimensions of the grains as a function of the initial platelet dimensions, after sintering. **d** Density of the greed bodies (blue) and the sintered ceramics (orange) as a function of the platelet and grain aspect ratio p, respectively

$$L_s^3 - L^3 = B \cdot e^{mT}, \tag{3}$$

where L is the initial template width and L_s the width after sintering, T the sintering temperature, and B and m constants are determined experimentally: $B = 3.969 \cdot 10^{-11}$ μm^3 and $m = 0.0175$ °C^{-1}. The dimensions of the templates measured after sintering were found to follow the prediction (Fig. 5c), whereas the thicknesses of the templates were found to be of 0.5 μm approximately for all platelet dimensions. Finally, the ceramic densities also varied as a function of the initial aspect ratios of the platelets (Fig. 5d). Although there was no direct correlation between the initial aspect ratio and the final density due to the simultaneous variation of length and thickness, the final densities did show correlation with the final aspect ratios of the grains. Indeed, higher aspect ratios corresponded to lower densities. This is probably due to the lower packing density of long grains as compared with smaller and rounder grains.

Deliberate Orientation Using Magnetic Fields

The orientation of the grains in the final ceramics were controlled by magnetically orienting the platelets in the liquid slurries using rotating magnetic fields (Fig. 6) [22]. In view of using the same set-up for all compositions, the five types of platelet should be able to align for the same magnetic field strength. To this aim, their magnetic coating was modified to allow their alignment under a magnetic field of 10 mT only. First, the theory of the magnetic alignment of anisotropic particles decorated with iron oxide nanoparticles of 10 nm diameter was applied [22] (Fig. 6a). This alignment results from the competition between viscous and magnetic torques when the particle rotates along with the magnet. Thus, it was predicted that at a constant particle diameter, a higher aspect ratio—hence a higher anisotropy was favorable for magnetic alignment. In this case, the magnetic susceptibility χ required for the platelets to orient with the field decreases. Since the magnetic susceptibility is the consequence of having Fe_3O_4 nanoparticles adsorbed on the surface, the minimum concentration of Fe_3O_4 decreases with the aspect ratio. On the contrary, at constant thickness, the viscous torque dominates when the diameter of the platelet increases demanding a higher magnetic susceptibility, hence an increase in Fe_3O_4 concentration. Following those predictions, the concentration of Fe_3O_4 needed was calculated so that all platelets align at 10 mT. The obtained magnetically responsive platelets were found to exhibit the predicted alignment when suspended in a low viscosity fluid under a rotating magnetic field at ~10 mT (Fig. 6b). The microscopic images and their FFT showed a very good biaxial orientation of the platelets according to the position of the magnetic field.

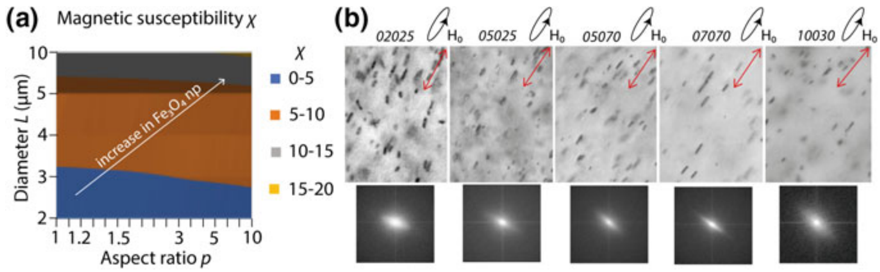

Fig. 6 **a** Theoretical determination of the magnetic susceptibility χ as a function of the diameter L of the platelet and their aspect ratio p to achieve magnetic alignment at 10 mT. The magnetic susceptibility is controlled by the concentration of Fe_3O_4 nanoparticles adsorbed at the surface of the Al_2O_3 platelets. **b** Optical images of aligned ceramic platelets suspended in low viscosity fluid and the fast Fourier transform (FFT) of the images (underneath)

Oriented and Multilayered Ceramics

MASC-TGG was applied to the slurries containing the magnetically responsive particles. The set-ups used for MASC-TGG are simple and offer a large range of variability in sample size, magnetic fields, and provide space for additional accessories such as microscope or temperature control (Fig. 7). The set-ups feature a rotating rare-earth magnet or alternatively a rotating sample, as well as the mold

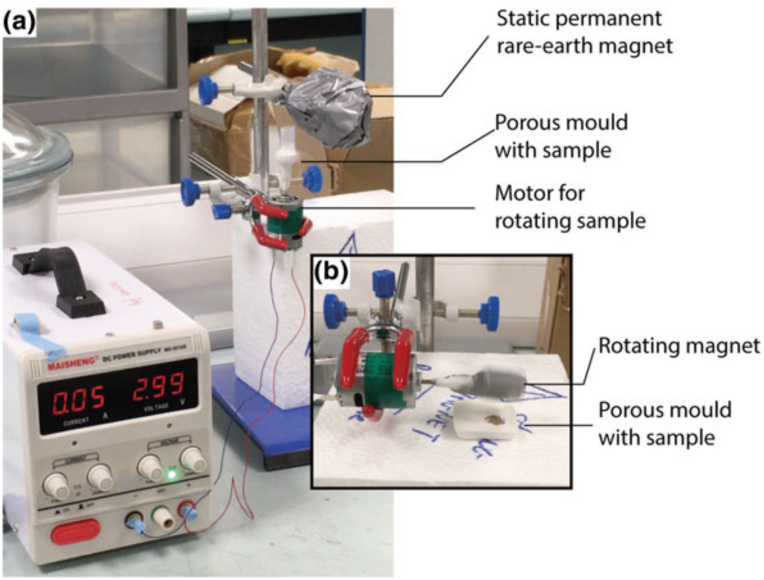

Fig. 7 Set-ups used for MASC-TGG for horizontal alignment (**a**) and for vertical alignment (**b**) of the Al_2O_3 templates

with the porous substrate. Thanks to the optimization of the slurries, the same set-ups could be used for all suspensions independently of the template size.

Using the magnetic alignment of the particles in the slurry, the green bodies as well as the sintered ceramics exhibited the intended microstructures (Fig. 8). First, it was verified that after MASC, the platelets were locked into the desired orientation set by the rotating magnetic field. This was done by choosing the least natural orientation of platelets, namely, biaxial vertical alignment (Fig. 8a). After MASC and drying of the samples, all compositions exhibited the intended vertical orientation of the platelets in the green body. The platelet alignment could be easily observed under electron microscopy after brittle fracture of the sample perpendicularly to the alignment direction. Indeed, in this case, some platelets were pulled out from the nanoparticles bed, leaving a gap that appears black under microscope. Using image analysis, the FFT of the micrographs confirmed the preferential orientation of those black features, hence a good vertical alignment (Fig. 8b). To exemplify how these slurries and the process could be used for heterogeneous bioinspired microstructured ceramic, a multilayer sample was prepared (Fig. 8c).

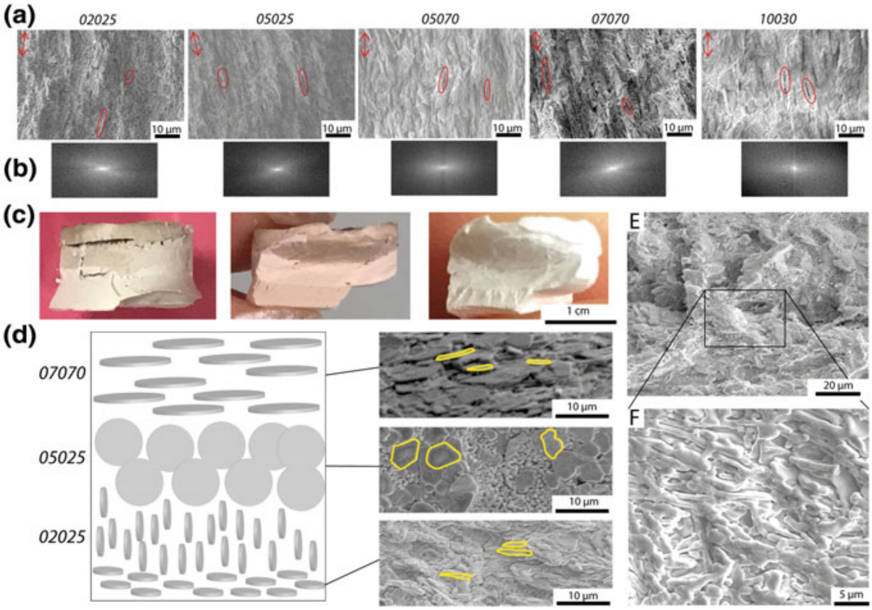

Fig. 8 **a** Electron micrographs of green bodies with vertical alignment of the Al_2O_3 platelets and the corresponding FFT **b** for the different template dimensions used. The red arrows in the images indicate the direction of the alignment of the grains, and the red ellipses circle the gaps left by platelets during the fracture revealing their orientation. **c** Pictures of a multilayer sample green bodies (left and middle) and after sintering (right). **d** Schematics of the grain orientation and particle dimensions used in the multilayer with the corresponding electron micrographs (right). Platelet contours are highlighted in yellow. View of the junction between the layers in the sintered sample before (**e**) and after polishing

In this sample, three slurries were selected, containing the platelets 02025, 05025 and 07070, and deposited from bottom to top in this order. Each of these slurries was casted sequentially after the liquid from the previous layer was evacuated by slipcasting. Due to the large thickness of each layer and the difference in magnetic coating of the platelets, the layered structure was visible optically in the green body with a change in color (Fig. 8c, left). The multilayering was more apparent after fracture of the green body in half (Fig. 8c, middle), whereas it disappeared in the sintered sample (Fig. 8c, right). The loss in color in the sintered sample can be attributed to the low concentration of iron oxide nanoparticles, whose atoms could diffuse into the alumina lattice with the high temperature sintering. Along with the change in composition, the ceramic was designed to have varying grain orientations between each layer, as schematized in Fig. 8d. It can be noted that the initial layer had two orientations. This is because slipcasting inevitably leads to the formation of a horizontally aligned layer close to the surface of the porous mold, due to the high capillary forces occurring there [14]. Corresponding electron micrographs showed the expected alignment. Finally, a closer look at the interface between the layers indicated good bonding without delamination (Fig. 8e, f). This may be attributed to the fact that after slipcasting, the sample is not entirely dried so that co-mixing by diffusion can still occur across the interface.

Conclusions

This study describes the preparation of a multilayered ceramics with simultaneous control of the local grain size, orientation, and porosity. The method employed template particles of various aspect ratios and dimensions that were modified to align in any deliberate orientation using external magnetic fields of same strength. Sequentially depositing layers containing different particle sizes and orientation, multilayered green bodies can be obtained. These green bodies were then sintered to allow for templated grain growth and densification. The final ceramic exhibited variations in local grain orientation and density, as intended by the design. Future research on this topic will involve the combination of selected suspensions with periodic microstructures of decreasing pitch, to more closely imitate the design of the Mantis Shrimp dactyl club and, hopefully, some of its outstanding properties. The ultimate motivation of the work is to obtain as strong but less brittle dense alumina ceramics.

Acknowledgements The author acknowledges financial support from Nanyang Technological University with the Start-Up grant M4082382.050).

References

1. Naleway SE, Porter MM, McKittrick J, Meyers MA (2015) Adv Mater 27:5455
2. Le Ferrand H, Bouville F, Niebel TP, Studart AR (2015) Nat Mater 14:1172
3. Le Ferrand H (2019) Compos Struct 224:111105
4. Wegst UGK, Bai H, Saiz E, Tomsia AP, Ritchie RO (2015) Nat Mater 14:23
5. Munch E, Launey ME, Alsem DH, Saiz E, Tomsia AP, Ritchie RO (2008) Science (80-.) 322:1516–80
6. Weaver JC, Milliron GW, Miserez A, Evans-Lutterodt K, Herrera S, Gallana I, Mershon WJ, Swanson B, Zavattieri P, DiMasi E, Kisailus D (2012) Science (80-.) 336:1275
7. Amini S, Masic A, Bertinetti L, Teguh JS, Herrin JS, Zhu X, Su H, Miserez A (2014) Nat Commun 5:1
8. Studart AR (2012) Adv Mater 24:5024
9. Barthelat F, Mirkhalaf M, Soc JR (2013) Interface 10
10. Nelson I, Naleway SE (2019) Integr Med Res 8:2372
11. Kokkinis D, Schaffner M, Studart AR (2015) Nat Commun 45:333
12. Le Ferrand H (2019) J Mater Res 34:169
13. Le Ferrand H, Bouville F (2019) J Am Ceram Soc 1
14. Le Ferrand H, Bouville F, Studart AR (2019) Soft Matter 15:3886
15. Seabaugh M, Messing GL (1997) J Am 88:1181
16. Pavlacka RJ, Messing GL (2010) J Eur Ceram Soc 30:2917
17. Habelitz S, Carl G, Russel C, Thiel S, Gerth U, Schnapp J-D, Jordanov A, Knake H (1997) J Non Cryst Solids 220:291
18. Suzuki TS, Sakka Y (2005) Scr Mater 52:583
19. Palmero P (2015) Nanomaterials 5:656
20. Bonderer LJ, Studart AR, Gauckler LJ (2008) Science (80-.) 319:1069
21. Suvaci E, Oh KS, Messing GL (2001) Acta Mater 49:2075
22. Erb RM, Segmehl J, Charilaou M, Löffler JF, Studart AR (2012) Soft Matter 8:7604
23. Erb RM, Libanori R, Rothfuchs N, Studart AR (2012) Science (80-.) 335:199